Green Chemistry

PAPER

View Article Online
View Journal | View Issue

Cite this: *Green Chem.*, 2024, **26**, 6822

Exploring the potential of regenerated lyocell fiber composites: a sustainable alternative for high-strength applications

Mahyar Fazeli, *[a] Shariful Islam,[a] Hossein Baniasadi, [b] Roozbeh Abidnejad, [a] Inge Schlapp-Hackl,[a] Michael Hummel [a] and Juha Lipponen[a]

Cellulose-based fiber-reinforced composites are gaining attention for their eco-friendly attributes and cost-effectiveness. However, their application in high-strength domains remains limited due to the dominance of synthetic and inorganic fibers. This study explores the potential of composites utilizing "lyocell fiber", a unique cellulose fiber, in comparison to carbon, cellulosic, and glass fiber composites. Our findings reveal that lyocell fiber composites exhibit earlier thermal degradation compared to carbon fiber composites according to thermogravimetric analysis (TGA). Analysis *via* scanning electron microscopy (SEM) highlights exceptional interaction between lyocell fiber and bio-based epoxy, surpassing other fibers. Additionally, assessment of composite hydrophilicity or hydrophobicity through contact angle measurements reveals distinctive surface characteristics, with lyocell exhibiting a contact angle of 80°, comparable to carbon fiber's contact angle of 75°, while glass transition results demonstrate lyocell fiber's transformation closely resembling that of carbon fiber composites. Although lyocell fiber exhibits lower strength (approximately 50 cN per tex) compared to carbon fiber (222 cN per tex), lyocell composites demonstrate promising strength levels nearly half that of carbon fiber composites (approximately 230 MPa for lyocell fiber composite compared to 500 MPa for carbon fiber composite). These results underscore the potential of lyocell composites as sustainable alternatives to petroleum-based and synthetic fiber composites, thus contributing to a more environmentally sustainable future.

Received 26th September 2023,
Accepted 15th April 2024

DOI: 10.1039/d3gc03637e

rsc.li/greenchem

1. Introduction

In response to the imperative to mitigate carbon emissions, industries are increasingly adopting biodegradable composites for various applications.[1,2] This trend has led to a surge in demand for composites, characterized by the use of natural cellulose fibers as reinforcement and bio-based polymers as matrices over the past several years.[3] According to the reports, the worth of composites reinforced with natural fibers was anticipated to be US$6.4 billion in 2022 and is expected to increase to US$14 billion by 2030. Another survey result depicted that the demand for natural fiber composite products will reach US$424 million in 2028 with a 5.3% growth rate.[4] However, natural fibers have substantial benefits compared to synthetic fibers and are gradually becoming popular in composite applications. Lignocellulosic fibers extracted from plants are currently gaining attention as potential reinforcements for polymer-matrix composites (PMCs). This interest stems from their abundant availability, cost-effectiveness, and biodegradability.[5] Natural fibers have attracted significant attention due to their environmentally friendly characteristics, contributing to sustainable practices.[6] The application of natural fiber composites has experienced substantial growth, particularly in industries such as construction, automotive, sports, bioengineering, aerospace, electrical and electronics, food packaging, and energy storage.[7–13] These fibers offer versatile and biodegradable solutions, known for their exceptional strength, lightweight nature, endurance, and environmental sensitivity.[14,15]

Within the context of natural fibers, there is an increasing awareness of environmental safety and the utilization of natural products in daily life. This trend is driven not only by considerations of low cost and raw material availability but also by a collective commitment to the well-being of both people and the planet.

As the demand for sustainable materials continues to rise, scientists are exploring synthetic alternatives with comparable qualities to natural fibers. The use of natural fiber-reinforced composites is gaining popularity, driven by their environmen-

[a]*Department of Bioproducts and Biosystems, School of Chemical Engineering, Aalto University, FI-00076 Aalto, Finland. E-mail: mahyar.fazeli@aalto.fi*
[b]*Polymer Technology, School of Chemical Engineering, Aalto University, Espoo, Finland*

tally friendly and biodegradable characteristics.[16] However, there is also a noteworthy shift in certain applications where synthetic fibers are replacing natural counterparts like jute, hemp, and flax. This transition is motivated by factors such as the lower cost, lightweight nature, reusability, and decomposability of synthetic fibers.[17,18] The increasing preference for natural fibers over synthetic ones aligns with their role as sustainable and biodegradable resources, making them ideal for the production of environmentally friendly composites. This transition towards biobased products, including biodegradable resources, bioenergy/biofuels, and environmentally friendly chemicals, represents a contemporary paradigm aimed at substituting petroleum-based materials. This shift is considered a crucial step towards a lower carbon economy, addressing global challenges related to renewable resource depletion and environmental concerns.[19]

While natural fibers offer advantages over synthetic and regenerated cellulose fibers, it is essential to acknowledge their drawbacks. One notable disadvantage is that natural fibers tend to be more hydrophilic and prone to moisture absorption, resulting in fiber swelling. This phenomenon can impact the interaction between the fiber and matrix, thereby influencing the strength properties of the composite.[20,21] The irregularity properties of regenerated cellulose fiber are insignificant compared to natural fiber. The other properties, for instance, fiber length, diameter, linear density, and strength, can be adjusted during the manufacturing process.[22,23] The main advantages of regenerated cellulose fiber as reinforcement material in the composite are its excellent uniformity, high tensile strength, good adhesion properties, and less defect.[24,25]

The use of regenerated cellulose fibers and textiles as strengthening elements has been the subject of numerous investigations in composites,[26,27] but until now, the required research has not been conducted on regenerated cellulose fabric produced by Ioncell technology. However, one research has been conducted using the Ioncell-F filament form in unidirectional composites. The author assessed how the proportion of volume and the characteristics of the fiber affect the mechanical properties of the composite,[28,29] whereas this study evaluates the potential of woven fabric structures and compared the properties of composite with high-strength carbon and glass fiber as well as commercial high-strength viscose fiber. Composites made from carbon fiber are not capable of breaking down naturally. The manufacturing process of carbon fiber discharges harmful pollutants into the atmosphere, potentially causing detrimental effects on the environment and human health. Furthermore, since carbon fiber does not decompose naturally, it is likely to accumulate in waste disposal sites after its usage.[30,31]

The primary objective of this investigation is to develop and assess a biodegradable cellulose composite with the potential to serve as a substitute for carbon fiber composites. The methodology employed involves the creation of a fabric utilizing Ioncell fiber, ensuring its structural equivalence to carbon fiber. Subsequently, a composite is developed using a bio-based epoxy through the vacuum infusion technique. The ensuing step involves a comprehensive comparison of mechanical, thermal, and morphological properties. This study further endeavors to comprehend the mechanisms facilitating enhanced fiber–matrix interaction for optimal mechanical properties, juxtaposing the Ioncell fiber composite with petroleum-based carbon and glass fibers, as well as other regenerated fibers (*e.g.*, viscose fiber). The manufacturing process route of composite is demonstrated in Fig. 1.

The execution of this study involved the utilization of Ioncell and viscose filaments for fabric weaving (plain weave) on a table loom. Various layers of Ioncell fabric composite, along with carbon fiber, glass fiber, and viscose/cotton fabric composites, were produced and subjected to a comparative analysis against commercial carbon, viscose, and glass fabric composites. Furthermore, diverse properties were rigorously assessed through a myriad of characterizations and tests, including tensile testing, thermogravimetric analysis (TGA), differential scanning calorimetry (DSC), scanning electron microscopy (SEM), and contact angle measurements.

2. Materials and methods

2.1 Materials

The Ioncell filament, derived from wood pulp, was generously provided by the Ioncell team at Aalto University.[32,33] Viscose filaments were sourced from CORDENKA GmbH & Co. KG, based in Obernburg, Germany. The carbon fiber textile, composed of polyacrylonitrile precursors (T700), was acquired from Easy Composites in the UK, while the glass fiber textile, consisting of alumino-borosilicate glass with less than 1% w/w alkali oxides, was supplied by OC 2400tex, Owens Corning, USA. Utilizing Ioncell and viscose filaments, fabrics were meticulously crafted on a weaving loom at the Bioproduct and Biosystem Department at Aalto University. For an in-depth analysis of fiber diameters, a scanning electron microscope was employed. Prior to the SEM examination, the fibers underwent coating with an 80 Au/20 Pd sputter coater to mitigate charge accumulation. Measurements were conducted across five different sections, and subsequent calculations yielded the average diameter.

Fiber analysis encompassing linear density, strength, and elongation was conducted using the Textechno Herbert Stein Favigraph instrument. This comprehensive study involved the utilization of five distinct types of fibers, each contributing to the fabrication of the woven fabric with an identical structure.

The bio-based epoxy resin utilized in this study (AMPRO™ BIO) was procured from Gurit, featuring a 40–60% bio-based system. Additionally, the corresponding slow curing agent was acquired from the same supplier. For the vacuum infusion process, a resin-to-hardener ratio of 3 : 1 was applied by volume, and the system exhibited the capability of curing at room temperature. Technical details regarding the epoxy resin and hardener, including essential specifications, are presented in Table 1 and sourced directly from the product manufacturer.

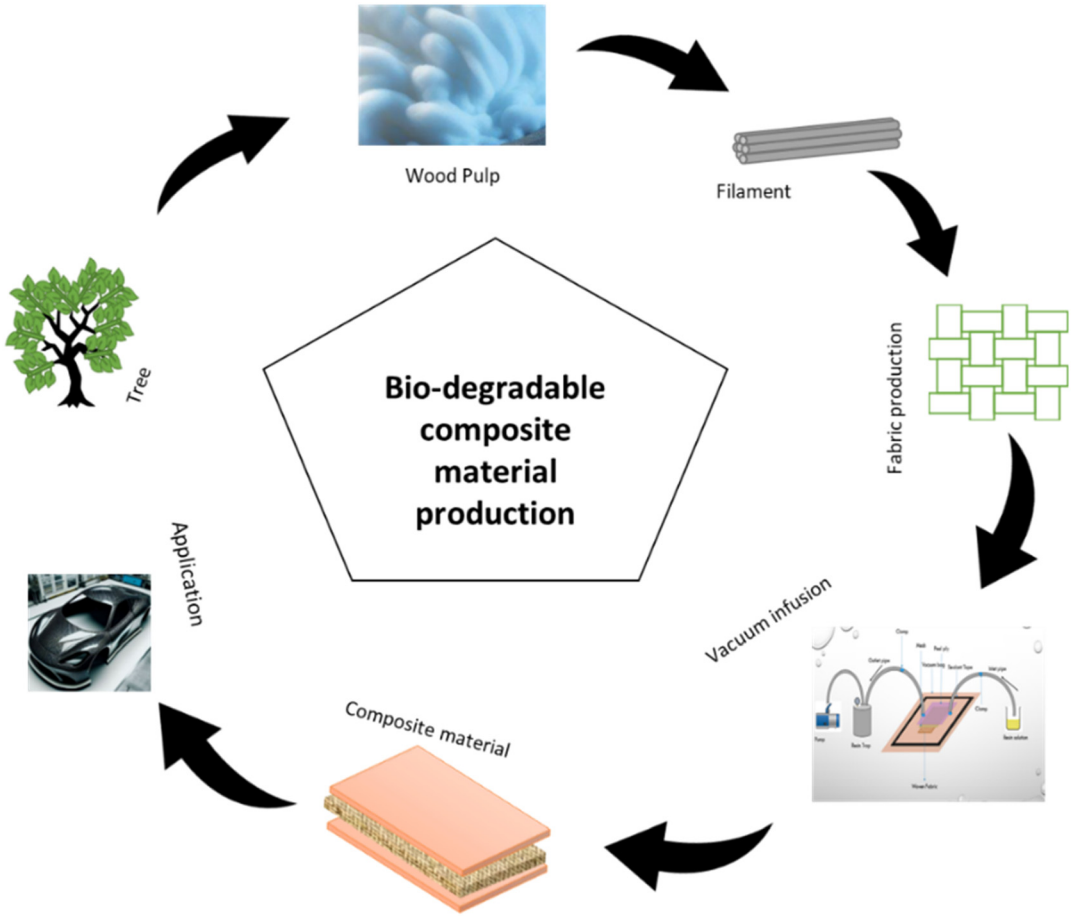

Fig. 1 Manufacturing process route of Ioncell fiber composites.

Table 1 Key properties of the bio-based epoxy resin system

Properties	Value
Tensile strength (MPa)	32.0
Mix ratio by volume	3 : 1
Density (g cm^{-3}) at 21 °C	1.1

2.2 Manufacturing of fabrics

The weaving process was executed on a Leena table loom obtained from Toika Oy, Finland. The filaments were meticulously threaded through the heddle eyes of the loom's harnesses. To guarantee a uniform fabric width, 10 cm intervals were marked on the reed for the strategic insertion of the warp filament. Ensuring the warp filaments' correct tension and averting yarn breakage, the filaments were securely fastened at both ends of the loom. Once the warp yarn was prepared, the weft yarn was loaded into the shuttle for seamless insertion through the warp yarn. Following the weft yarn insertion, the beating-up process was carried out carefully, compacting the weft yarn with the warp yarn to establish the desired fabric structure. The fabrics were woven in a plain weave pattern with a 1 × 1 structural design, as illustrated in Fig. 2.

2.3 Manufacturing of composites

The production of biodegradable Ioncell fiber and other fiber composites was achieved through the application of the vacuum infusion method, a state-of-the-art and environmentally conscious approach in composite manufacturing. This technique enables the homogeneous infusion of the matrix throughout the reinforcing fabric, fostering superior interfacial bonding between the matrix and fiber when compared to alternative composite production methods. The fabrication process involves the placement of the fabric onto a glass mold, followed by the arrangement of a peel ply, breather ply, and vacuum bag atop the fabric.

The glass mold is equipped with two tubes, one designated for resin supply and the other serving as an outlet for the resin-to-resin trap. A vacuum pump is connected to the resin trap, and the setup is secured with multiple clamps. The inlet clamp precisely governs the controlled supply of resin to the material. The operational configuration during composite production is visually represented in Fig. 3. Following the completion of the setup, the motor is activated, ensuring a secure vacuum with no leaks. The prepared matrix is then connected to the inlet pipe, and the clamp is opened, initiating the resin infusion through the reinforced fabric. The infusion process

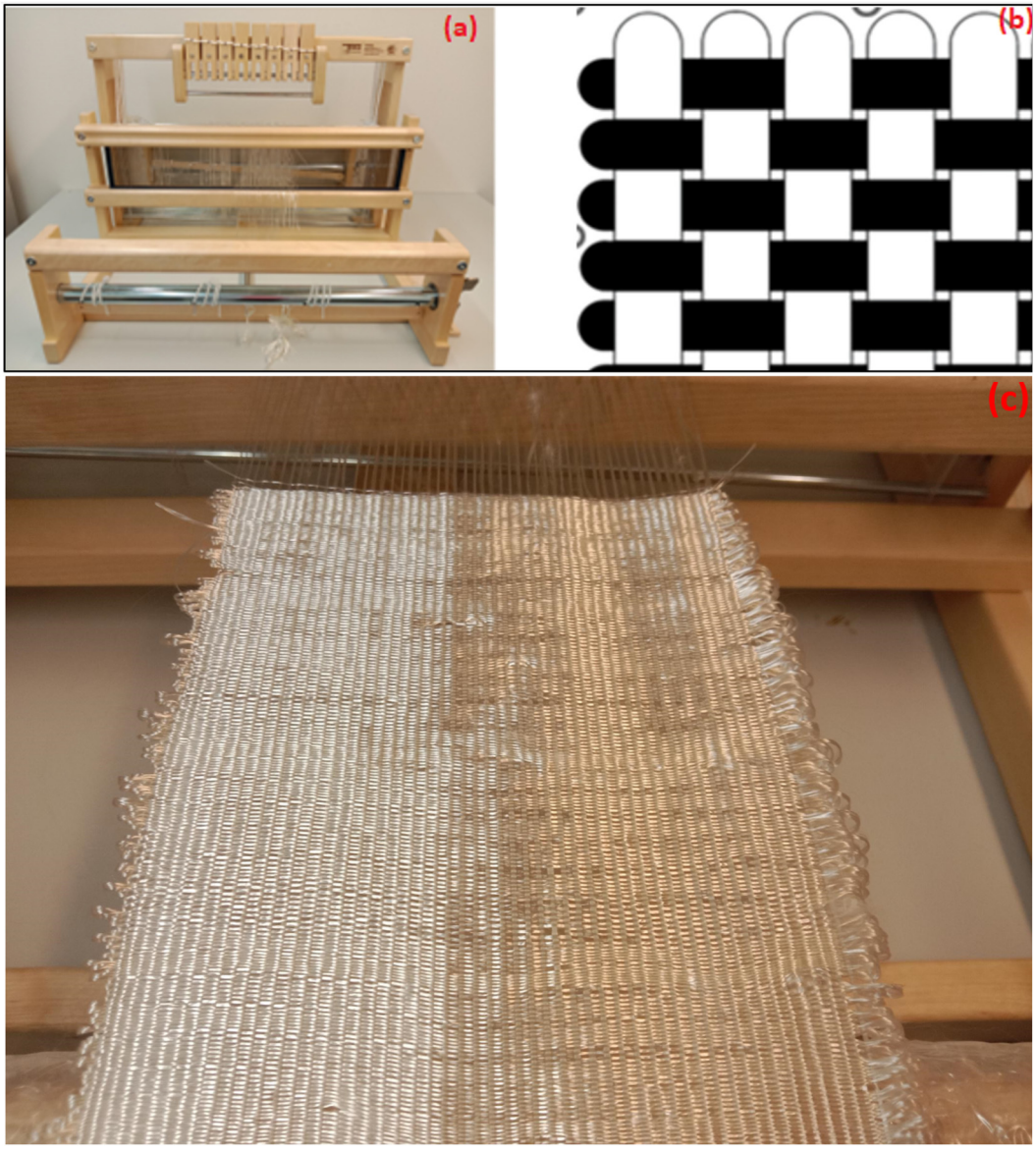

Fig. 2 Fabric weaving process: (a) weaving loom and (b) 1 × 1 plain weave structure. (c) Ioncell fabric manufactured in this study.

spans approximately 5–7 minutes for each composite, culminating in the thorough impregnation of resin. Subsequently, the composite undergoes a curing period at room temperature for a minimum of 6 hours, ensuring the realization of optimal material properties. The sample codes of the prepared composites are CFRC for carbon fiber reinforced composite, GFRC for glass fiber reinforced composite, IFRC Ioncell fiber reinforced composite, VCFRC for viscose/cotton fiber-reinforced composite, and VFRC for viscose fiber reinforced composite.

2.4 Single fiber tensile properties of the samples

The tensile strength of individual filaments of Ioncell, carbon, glass, and viscose fibers was determined employing the vibroscopic method (Instrument-Textechno Herbert Stein GmbH & Co. KG), adhering to the principle of a constant rate of extension. The testing procedure followed the international standard method EN ISO 5079, with EN ISO 139 utilized for conditioning. Prior to testing, the fibers underwent conditioning in a standard atmosphere (65% RH) and temperature (20 °C) for 24 hours, in accordance with the standard method. A single filament was meticulously isolated from the multifilament using tweezers and a black/white board. This isolated filament was then securely clamped with a preselected tension weight and positioned within the testing device. A gauge length of 20 mm was established, employing a twenty cN load cell. A pretension weight of 100 mg, based on the linear density of the fiber, was applied. The testing speed was set at 1 mm min^{-1}.

2.5 Scanning electron microscopy

Microstructure analysis of the fibers is carried out using a scanning electron microscope (Sigma VP; Zeiss, Oberkochen, Germany) operating at an acceleration voltage of 5 kV.

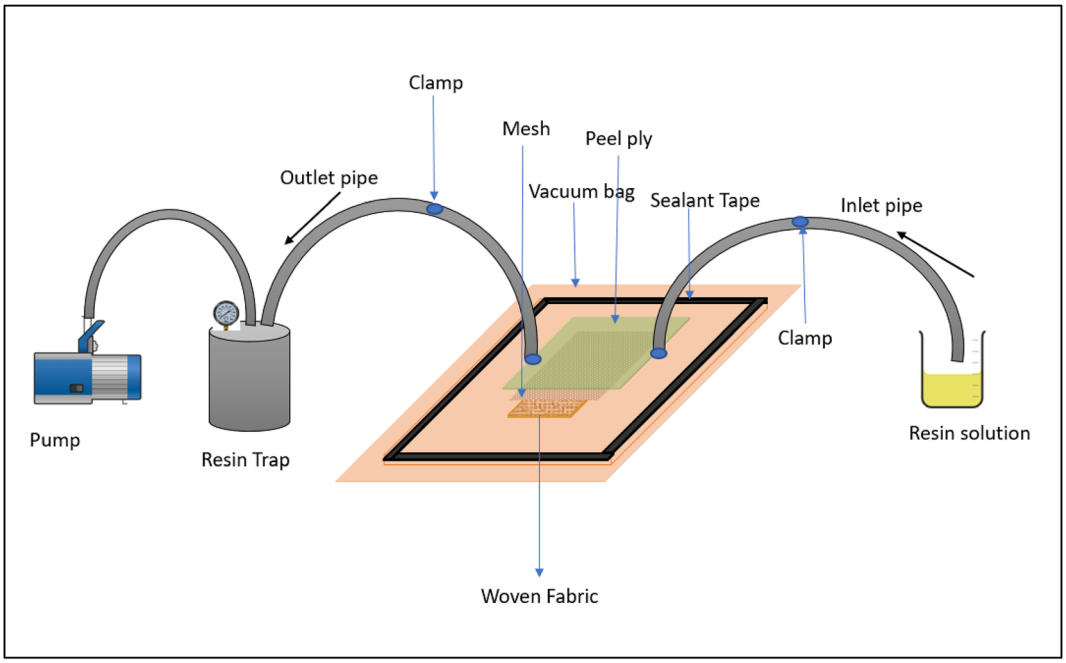

Fig. 3 Schematic diagram of the vacuum infusion process used in this study for composite fabrication.

Likewise, SEM is employed to inspect the fracture surfaces of the composites after undergoing tensile tests with an acceleration voltage of 3 kV. Before the examination, all specimens are coated with a 5 nm layer of gold using the high vacuum deposition technique (EM SCD500, Leica, Germany).

2.6 Wettability of fabricated composites

The analysis of composite wettability was carried out utilizing the "Theta Flex optical tensiometer", which measured the contact angle of the composite surface. The Theta Flex system integrates a video camera, an automatic XYZ sample stage, a dual dispenser unit, and an LED light source. The OneAttension software facilitated the smooth operation of the experimental process, providing flexibility in manipulating parameters. For this investigation, the sessile drop method, selected for its convenience in analyzing the surface properties of solid materials, was employed.

The experimental procedure commenced with an initial calibration to ensure accuracy before sample analysis. Following successful calibration, the water bottle was positioned on the surface of the automatic XYZ stage, with adjustments made to the stage and dispenser height to ensure precise water droplet placement. Subsequently, the sample was placed on the stage, and the program was initiated, causing water droplets to descend onto the composite surface. A USB3 camera captured a high-resolution image, enabling a detailed examination of the wettability characteristics.

2.7 Thermal analysis of the composites

The thermal characteristics of the composite were systematically analyzed employing thermogravimetric analysis (TGA) and differential scanning calorimetry (DSC). The Netzsch STA 449 F3 Jupiter & QMS 403 Aëolos Quadro instrument was utilized for TGA assessments. Initially, specimens were encapsulated in 85 μL Al_2O_3 crucibles (Netzsch) and subjected to a controlled temperature ramp from 40 to 800 °C at a heating rate of 10 °C under a gas flow of 70 mL min^{-1}, composed of 15 vol% oxygen and a blend of 50 mL min^{-1} air and 20 mL min^{-1} nitrogen.

The DSC (TA Instruments Discovery DSC) facilitated the determination of the glass transition temperature of the composite. Additionally, the melting temperature and crystallinity degree of thermoplastic composites were evaluated within a temperature range spanning −50 °C to 250 °C. The heating/cooling rate was set at 10 °C min^{-1}. Sample masses, ranging between 5–14 mg, underwent meticulous preparation, including slicing, weighing using a precision balance, and placement in dedicated aluminum pans. Subsequent to covering the sample with a top pan and ensuring secure sealing, a reference sample was concurrently analyzed for comparative purposes.

2.8 Tensile test of composites

The tensile properties of the produced composites, including tensile strength, Young's modulus, and elongation at break, are analyzed using a Universal Testing Machine (Instron, MTS 4204, United States). This analysis aimed to investigate the performance of composites reinforced with different fibers. Six dog-bone specimens for each kind of composite are cut by a waterjet cutting machine (JJ-I, Shanghai Jinjian, China) based on ISO 527-4(1A). The average dimension of each specimen is approximately 150 mm × 20 mm × 4 mm. The tensile test is

conducted at room temperature and 50% relative humidity using a testing speed of 1 mm min^{-1}. A load cell of 5 kN is employed to determine the tensile strength and Young's modulus of all the prepared samples. Additionally, the strain at breaks is measured using an extensometer attached to one side of the sample, with a gauge length of 50 mm.

3. Results and discussion

3.1 Morphology of fibers

Fig. 4 illustrates the surface characteristics of Ioncell, viscose, glass, and carbon fibers, providing valuable insights into their morphological attributes. SEM imaging reveals distinctive features of each fiber type. The Ioncell fiber surface exhibits a remarkably smooth and rod-like structure, consistent with observations from prior studies.[34] This surface morphology is indicative of the unique characteristics of Ioncell fibers, showcasing their refined and uniform composition. In contrast, the surface analysis of viscose fiber reveals a more irregular and jagged edge characterized by fine lines that traverse its length. This distinct surface texture highlights the heterogeneous nature of viscose fibers, presenting a stark contrast to the smoother profile of Ioncell fibers. Interestingly, both glass and carbon fibers exhibit a rod-like structure akin to Ioncell fibers, showcasing a notable similarity in their morphological features. The absence of fine lines along the longitudinal axis of both glass and carbon fibers aligns with the smooth and con-

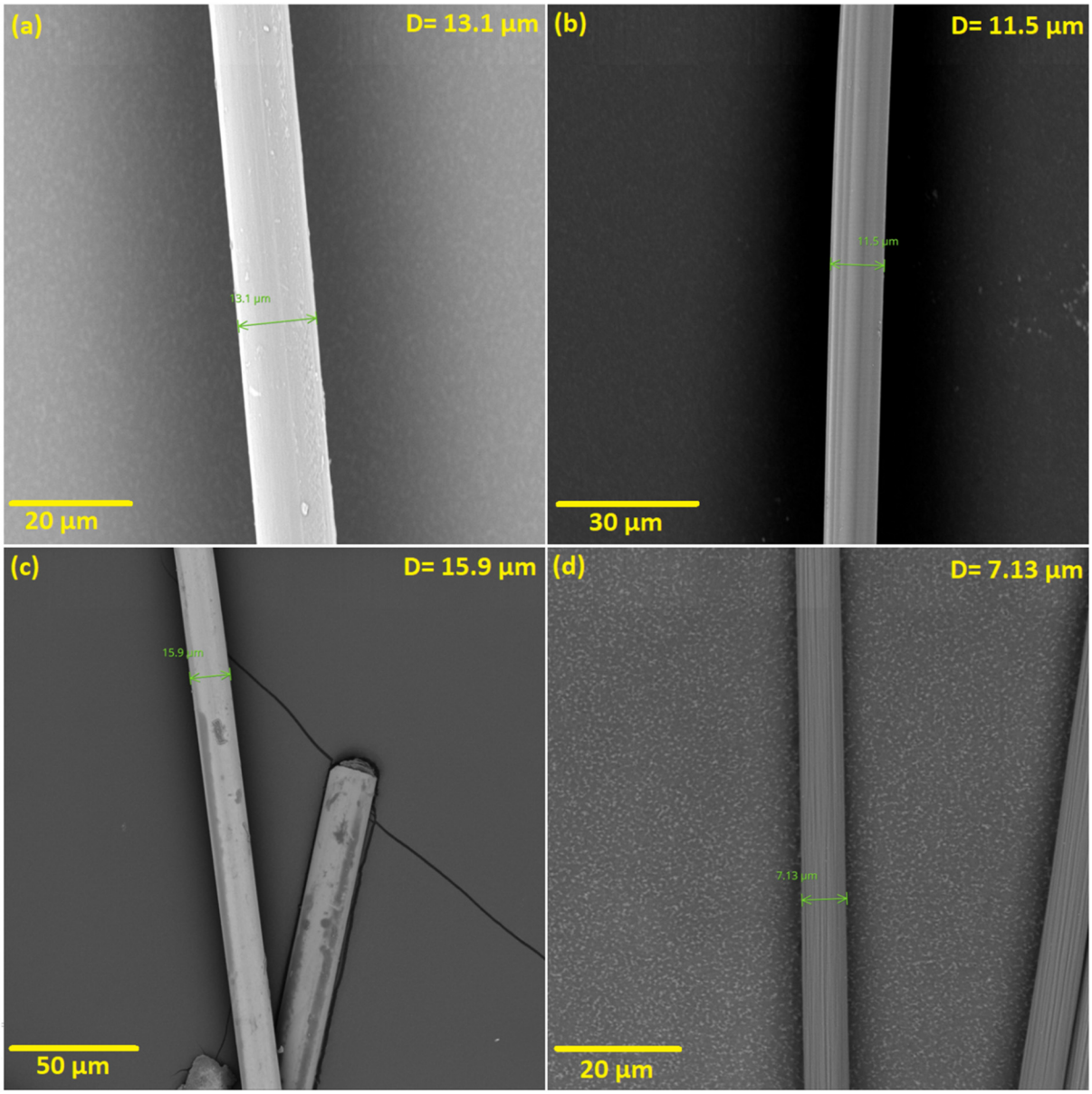

Fig. 4 SEM images of (a) Ioncell, (b) viscose, (c) glass, and (d) carbon fiber.

tinuous nature observed in Ioncell fibers. This consistency in rod-like structure suggests commonalities in the fundamental morphological aspects of these high-strength fibers. These detailed surface analyses contribute to a comprehensive understanding of the morphological distinctions among Ioncell, viscose, glass, and carbon fibers. Such insights are crucial for elucidating the unique characteristics and potential applications of these fibers in various composites, thereby advancing the knowledge base in the field of fiber-reinforced composites.

3.2 Single fiber tensile properties

The tensile properties of the fibers were determined by separating the fiber from the continuous multifilament. A long filament was cut into small pieces of 30 mm, which is suitable to grip between the clamps. Linear density as well as elongation of cellulosic fiber (Ioncell and viscose) showed a higher value than the carbon fiber (Table 2). Meanwhile, the tenacity of carbon fiber is high (nearly 4.4 times that of cellulose fiber) compared to Ioncell and viscose fiber. Carbon fibers have a high strength-to-volume ratio because they are made of carbon atoms that are bonded together in crystals along the fiber axis. The strength of the cellulose structure is directly proportional to crystallinity and total orientation of its chains. Lower tensile strength and modulus are typically combined with a higher elongation at break.[35] The tenacity for carbon fiber was 222.24 cN per tex, but elongation and linear density were 2.41% and 0.65 dtex (deci-tex: Grams per 10 000 metres of yarn), respectively, which is lower than the cellulosic fiber.

The fiber's tenacity depends on several factors. For instance, degree of polymerization, bonding between adjacent polymer chains in the molecule, degree of orientation in the fiber axis as well as crystallinity. On the other hand, the elongation of fiber will be lower if the crystallinity is high, the orientation of the chain of polymer is higher as well as the durable bonding between inter-chains.[36]

3.3 Volume fraction of composites

All composite samples were composed of two fabric layers, and the calculated values for fiber volume fraction, matrix volume fraction, fiber weight fraction, matrix weight fraction, and composite density are summarized in Table 3. Analysis of the data reveals that the carbon fiber-reinforced composite exhibits the highest volume fraction, followed by the viscose fiber-reinforced composite and the glass fiber-reinforced composite. Conversely, the Ioncell fiber-reinforced composite shows the lowest fiber volume fraction, with the viscose/cotton fiber-reinforced composite closely following. Interestingly, the composite density is lowest for the viscose/cotton fiber-reinforced composite, succeeded by the Ioncell fiber-reinforced composite. In contrast, the glass fiber-reinforced composite exhibits the highest density among the tested composites.

3.4 Wettability of the composites

The assessment of composite hydrophilicity or hydrophobicity involves measuring the surface contact angle, which not only provides insights into the material's water-attracting or repelling properties but also serves as an indicator of surface smoothness. Each sample underwent three contact angle measurements at different locations to ensure robust evaluation. Fig. 5 illustrates the contact angles of various composites, emphasizing the dependence of the contact angle on the nature of the reinforcing material. Previous research has demonstrated that a lower fiber content correlates with reduced water absorption rates, influencing the contact angle accordingly. Consequently, decreasing water absorption percentages may lead to an increase in the contact angle.[37,38]

Notably, the contact angle results for composites offer insights beyond hydrophilic or hydrophobic characteristics; they also provide valuable information about surface roughness or smoothness. This distinction is particularly evident in the case of carbon and glass fiber-reinforced composites. The

Table 2 Characteristics of fibers utilized in the study

Fiber	Diameter (μm)	Linear density (dtex)	Tenacity (cN per tex)	Young's modulus (cN per tex)	Elongation (%)
Ioncell fiber	13.1 ± 0.8	2.35 ± 0.2	50.16 ± 1.4	1676.4 ± 10.2	8.99 ± 0.2
Viscose fiber	11.5 ± 0.5	1.84 ± 0.3	51.53 ± 1.6	1077 ± 13.2	14.01 ± 0.4
Glass fiber	15.9 ± 0.7	0.95 ± 0.09	200.2 ± 4.1	9443.3 ± 9.8	2.12 ± 0.3
Carbon fiber	7.13 ± 0.7	0.65 ± 0.1	222.25 ± 3.2	9221.5 ± 5.3	2.41 ± 0.2

Table 3 Fiber volume fraction (FVF), matrix volume fraction (MVF), weight fraction of fiber (WFF), weight fraction of matrix (WFM), and composite density (CD)

Sample	FVF (%)	MVF (%)	WFF (%)	WFM (%)	CD (g cm^{-3})
GFRC	54.66 ± 1.3	45.34 ± 1.1	73.18 ± 1.3	26.82 ± 1.5	1.86 ± 0.05
VCFRC	45.40 ± 0.5	54.60 ± 0.7	53.46 ± 1.2	46.54 ± 1.2	1.29 ± 0.03
VFRC	56.12 ± 1.5	43.88 ± 1.2	63.87 ± 1.3	36.13 ± 0.8	1.34 ± 0.04
IFRC	51.33 ± 1.6	48.67 ± 1.1	59.31 ± 1.6	40.69 ± 1.4	1.32 ± 0.04
CFRC	60.38 ± 1.2	39.62 ± 0.9	70.92 ± 1.2	29.08 ± 0.9	1.50 ± 0.05

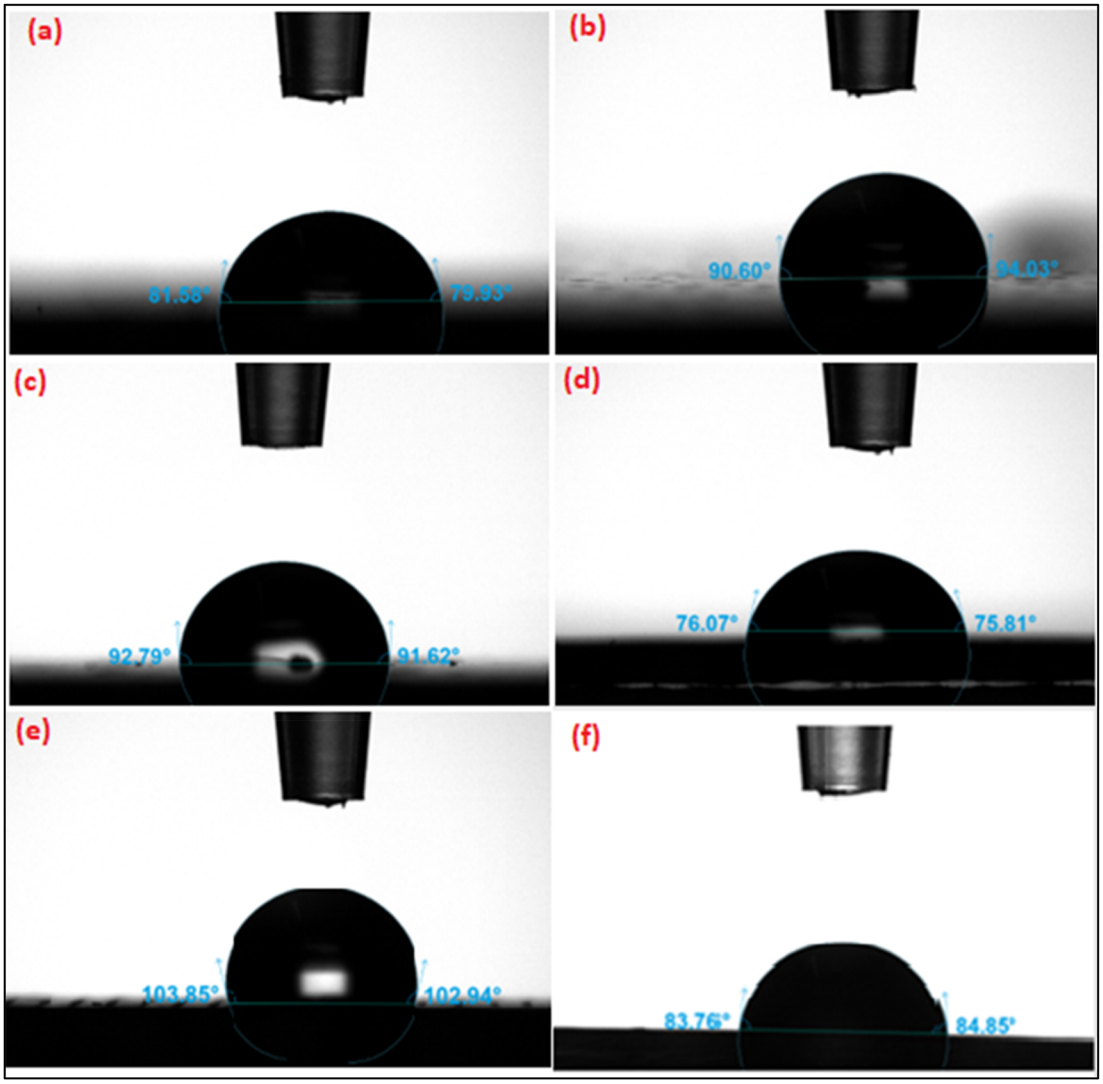

Fig. 5 Dynamic contact angle of (a) Ioncell fiber reinforced composite, (b) viscose fiber reinforced composite, (c) glass fiber reinforced composite, (d) carbon fiber reinforced composite, (e) viscose/cotton fiber reinforced composite, and (f) cured resin.

contact angle measurements for these materials contribute to a nuanced understanding of their surface characteristics, shedding light on aspects beyond the water interaction and advancing our comprehension of the intricate interplay between composition and surface properties in the composites.

The measured contact angles reveal distinctive surface characteristics, with the lowest contact angle observed in the carbon fiber-reinforced composite at 76.07°, closely followed by the Ioncell fiber-reinforced composite at 77.69° (Table 4). This proximity in contact angles between carbon and Ioncell fiber-reinforced composites suggests a comparable nature in the surface smoothness of these materials. In contrast, the contact angle for the viscose fiber-reinforced composite was found to be 92.31°, while the viscose/cotton blended fiber-reinforced composite exhibited a contact angle of 103.85°. Notably, the contact angles of natural fiber-reinforced composites, specifically those reinforced with hemp and flax fibers, fell within the range of 58–70°.[39] Additionally, an exploration of the contact angle of composites with rough surfaces demonstrated higher contact angles in areas with surface roughness.[40] Consequently, the carbon and Ioncell fiber-reinforced composites exhibit smooth surfaces, as evidenced by their relatively lower contact angles, while the viscose fiber-reinforced

Table 4 The dynamic contact angle (CA) of composites and neat epoxy resin

Sample	CA left	CA right	Average CA
CFRC	76.07	75.81	75.94
IFRC	81.58	79.93	80.75
GFRC	92.79	91.62	92.20
VFRC	90.60	94.03	92.31
VCFRC	103.85	102.94	103.39
Resin	83.76	84.85	84.30

composite approaches 90° and the viscose/cotton fiber composite surpasses the 90° threshold. These results indicate that the latter two materials possess rougher surfaces compared to the smoother profiles of the carbon and Ioncell fiber-reinforced composites.

3.5 Thermogravimetric analysis (TGA)

Fig. 6a represents the TGA curves of carbon, glass, Ioncell, viscose/cotton, viscose fiber reinforced composite as well as the neat Ioncell and epoxy resin. Furthermore, the detailed results of the derivative thermogravimetric (DTG) peak, onset temperature as well as residual mass percentage are presented in Table 5. The weight loss percentage was observed to be the lowest for glass fiber composite, which was 29.11%, whereas carbon fiber was 37.39%. On the other hand, all cellulosic fiber weight loss percentage was observed to be almost similar (IFRC-82.47%, VCFRC-84.11% as well as VFRC 81.8%). In contrast, the neat Ioncell and neat epoxy resin showed higher mass loss than the composite. It can be concluded that the mass loss percentage is less for the composite than the neat material with the same temperature. The maximum mass loss was observed between temperatures 300–400 °C for all the composites as well as neat material.

Fig. 6b shows the DTG curve, indicating the point of most significant mass loss. It was observed that cellulosic fiber and composite have small peaks before 100 °C which is related to the water evaporation.[41] The neat Ioncell-F was noted to have the most significant mass loss at a temperature of 338.6 °C and at a rate of 24% min^{-1}, which is nearly identical to the temperatures recorded for the GFRC was observed at 338.7 °C; however, the rate was 3.13% min^{-1} and carbon fiber composite rate was 4.1% min^{-1}. On the other hand, two peaks were observed for the CFRC, VFRC, neat epoxy resin, and VCFRC which indicates that the mass loss process happened in two stages. The first stage of mass loss was 333.7 °C, 310.2 °C, 314.9 °C, 304.7 °C consecutively. In contrast, the second stage of mass loss was slightly lower than the first stage, which was observed at 342.1 °C, 316.0 °C, 317.2 °C, and 328.3 °C. It can be deduced that all neat Ioncell-F, IFRC, and GFRC mass loss happened in one stage, whereas the CFRC, VFRC, neat epoxy resin, and VCFRC mass loss happened in two stages. From the curve temperature of neat fiber and neat epoxy resin, it can be concluded that resin was degraded at the first stage and fiber was degraded at the second stage. The rapid mass loss of Ioncell can be attributed to its monomeric nature, whereas the slower thermal degradation of cellulose or resin is linked to their polymer structures. Complex polymer molecules typically necessitate more time to ignite and burn.

Table 5 Thermal analysis data of different composites

Sample	DTG peak (°C)	DSC onset (°C)	Residual mass (%)	WFF (%)
CFRC	333.7	336.3	62.61	70.92 ± 1.2
IFRC	309.8	284.7	17.53	59.31 ± 1.6
GFRC	338.7	324.5	70.89	73.18 ± 1.3
VFRC	310.2	300.2	18.20	63.87 ± 1.3
VCFRC	304.7	286.1	15.89	53.46 ± 1.2
Neat resin	314.9	311.5	6.13	—
Neat Ioncell-F	338.6	314.1	10.22	—

3.6 Differential scanning calorimetry (DSC)

The DSC thermograph of carbon, Ioncell, glass, and viscose fiber composite and resin, ranging from −50 °C to 250 °C, is depicted in Fig. 7. The lower plot in the DSC graph indicates the endothermic phase, where heat is absorbed, while the rise signifies the exothermic phase, where heat is discharged.[42] It was noted that the glass transition temperatures for composites reinforced with cellulosic fibers, specifically 39.93 °C for

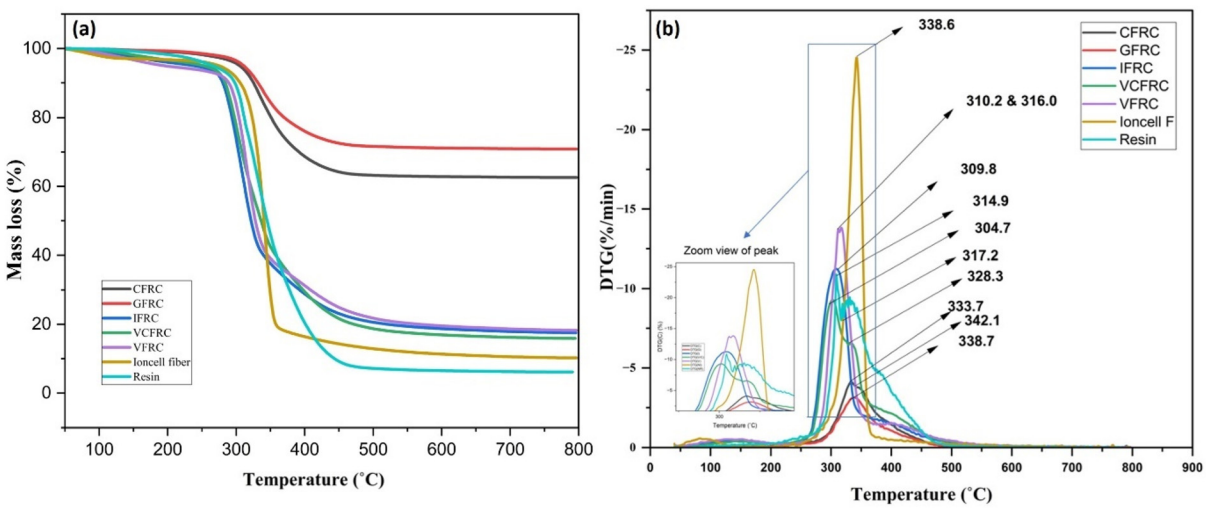

Fig. 6 (a) TGA and (b) DTG thermograms of carbon fiber reinforced composite (CFRC), glass fiber reinforced composite (GFRC), Ioncell fiber reinforced composite (IFRC), viscose/cotton fiber-reinforced composite (VCFRC), viscose fiber reinforced composite (VFRC), Ioncell fiber (Ioncell F), and neat resin.

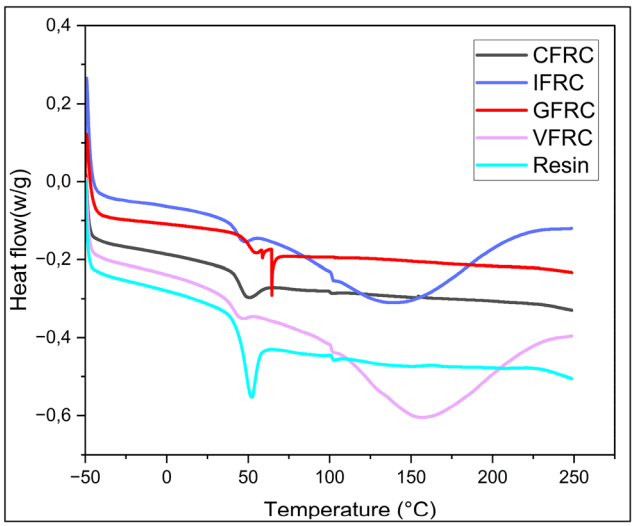

Fig. 7 Glass transition temperature from DSC curve of CFRC, GFRC, IFRC, VFRC, and neat epoxy resin.

IFRC and 37.91 °C for VFRC, are quite similar due to crystallinity and crystal structure of the regenerated cellulose. However, the T_g for composites reinforced with inorganic fibers is marginally higher than that of the cellulose fiber composite. The reported T_g for carbon and glass fiber composites are 42.46 °C and 51.75 °C, respectively. Interestingly, T_g for the neat resin was found to be slightly higher than that of the cellulose fiber composite. Several factors, such as the moisture content and the internal stress induced in the material, can influence thermal behavior during the process. This could be due to weak interface compatibility between the fiber and matrix, which allows for greater mobility of the epoxy molecular chain along the interface region, potentially resulting in a lower T_g.[43,44] Therefore, it can be deduced that the reduced mobility of the epoxy molecular chain in the interface region for carbon and glass fiber composite results in an elevated glass transition temperature. The glass transition temperature (T_g) of the resin decreases in all composites, with minimal impact observed in the case of glass fibers. However, cellulose fibers exhibit the most significant effect on the reduction of T_g. This effect is likely attributed to the high hydrophilicity of

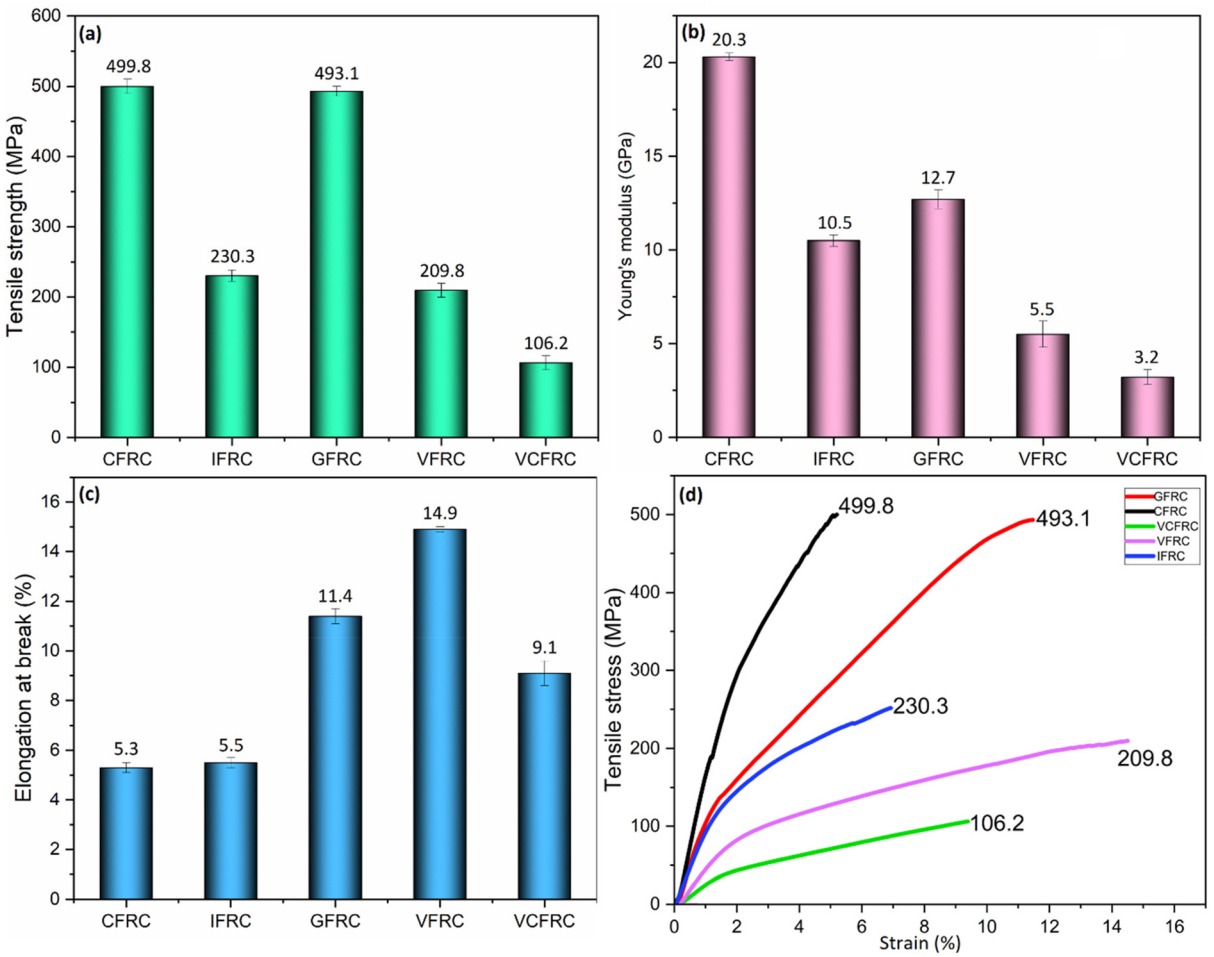

Fig. 8 (a) Tensile strength, (b) Young's modulus, (c) elongation at break, and (d) stress–strain curve of the fabricated composites.

cellulose, resulting in higher moisture content within the composites, as discussed by the authors.

3.7 Tensile testing of the composites

In the assessment of strength properties, this study explores the efficacy of various cellulosic fibers, including Ioncell, viscose, and cotton, as reinforcement within composites alongside inorganic fibers like carbon and glass. Five distinct composites were meticulously fabricated using a vacuum infusion process with a bio-based epoxy matrix. The resulting maximum tensile stress–strain curve, as depicted in Fig. 8, highlights the superior tensile strength of the carbon fiber-reinforced composite, albeit with a relatively lower strain compared to other composites. The investigation into the underlying factors influencing this disparity in strength and strain characteristics has been explored in prior research.[45]

The remarkable tensile strength of carbon fibers is attributed to their inherent rigidity and robustness. Fibers characterized by high strength typically exhibit an exceptionally elevated tensile strength coupled with a notable failure strain. In this

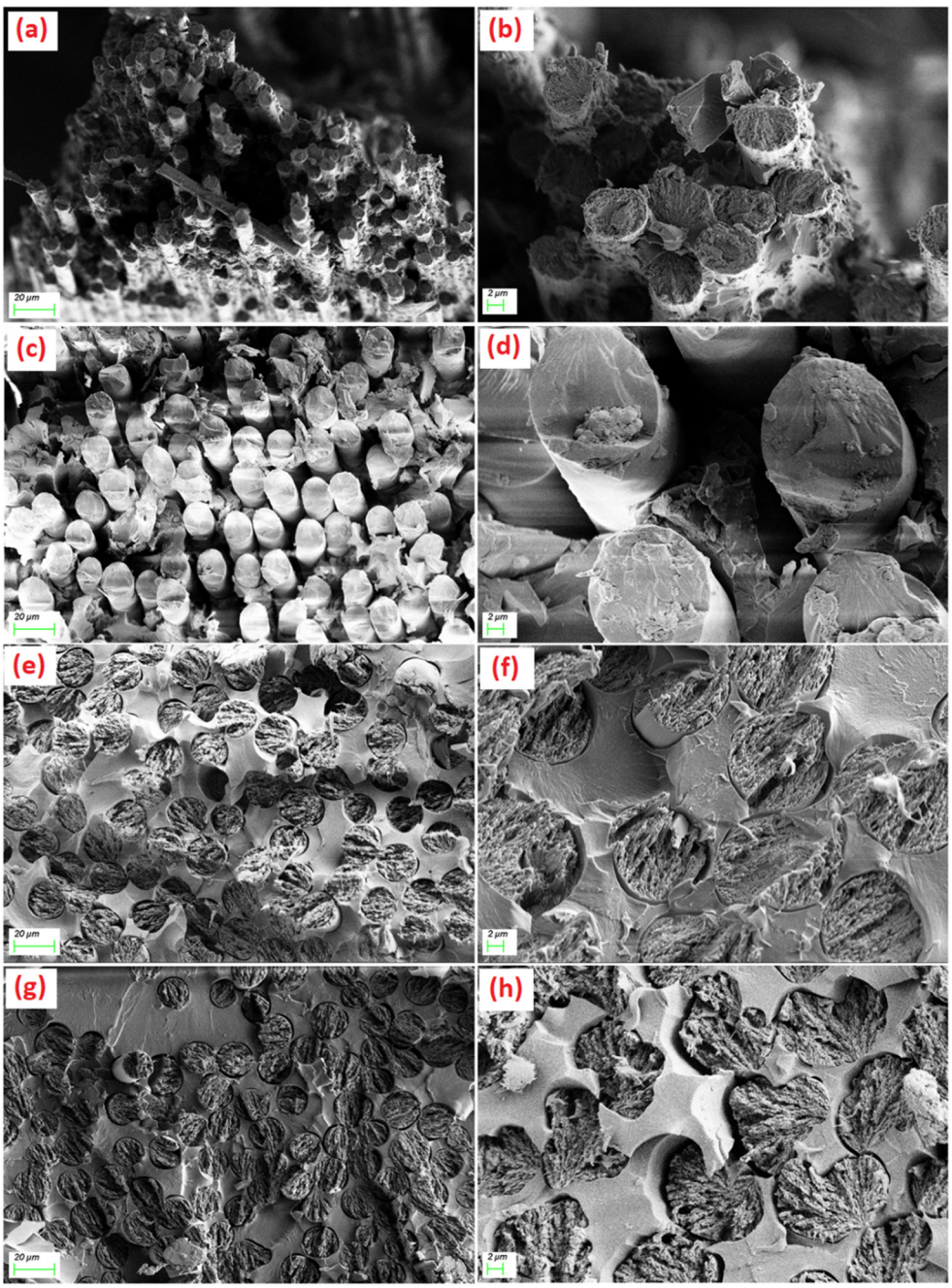

Fig. 9 SEM images of fractured surface after tensile test for (a, b) carbon fiber, (c, d) glass fiber, (e, f) Ioncell fiber, and (g, h) viscose fiber reinforced composites.

context, the Ioncell fiber composite demonstrated a tensile strength of 230.3 MPa, nearly half of that observed in carbon and glass fiber composites, yet 1.09 times higher than commercially available high-strength viscose fiber composites. The stress–strain curve analysis reveals an approximately linear behavior for carbon, glass, and Ioncell fiber-reinforced composites up to a yield stress of 90 MPa, indicating that the initial stress response of Ioncell fiber closely mirrors that of carbon fiber. The observed strength of the composite is intricately linked to the properties of both the reinforcement and matrix materials, emphasizing the pivotal role played by the interaction between these components.[46,47] This holistic investigation provides valuable insights into the nuanced interplay of materials within composite structures, contributing to a comprehensive understanding of their mechanical performance and facilitating informed material selection for diverse applications.

3.8 Fractography

All tested samples underwent longitudinal fracture during the tensile test, revealing distinct fracture behaviors and highlighting the intricate interaction between the matrix and fibers. SEM images captured at various magnifications offer detailed insights into the fractured surfaces. The inorganic fiber-reinforced composites, specifically carbon and glass composites, exhibited uneven fracture surfaces. In Fig. 9a and b, representing the fractured surface of the carbon fiber composite, ruptured fibers were observed, but the interaction between the fiber and matrix was not deemed poor. Some fibers fractured at the edge of the fracture area, while others broke in the middle, a phenomenon attributed to the inherent brittleness of the fibers. Matrix debris surrounding carbon fibers indicated matrix delamination from the fiber surface. Notably, no debonding or fiber pull-out was observed, indicating the absence of crack propagation. Fig. 9c and d reveals the fractured surface of the glass fiber-reinforced composite (GFRC), displaying adhesive and cohesive failures. The non-planar, rough failure surface indicates poor matrix and fiber interaction. Matrix debonding was evident, although no fiber pull-out was observed.

In contrast, the fractured surface of the Ioncell fiber-reinforced composite, as depicted in Fig. 9e and f, showcased excellent fiber–matrix interaction. The fibers exhibited uniform breakage without evidence of debonding or pull-out, and no instances of adhesion or cohesion failure were observed. This finding aligns with a similar observation reported in prior studies,[48] underscoring the robust compatibility between the matrix and Ioncell fibers, a critical factor influencing mechanical properties. Comparatively, the fracture surface of the viscose fiber composite (VFRC) is presented in Fig. 9g and h, where the cross-sectional shape of viscose fibers deviates from the circular profiles of Ioncell, carbon, and glass fibers. The compatibility between viscose fibers and the matrix material was deemed insufficient, resulting in poor adhesion. Although no cohesion failure was identified in the fractured area, gaps between the matrix and fibers suggested suboptimal interaction between the fiber and matrix materials.

4. Conclusions

In conclusion, this study aimed to assess the potential of Ioncell fiber as a substitute for carbon and other synthetic and cellulosic fibers, investigating its interaction with bio-based epoxy resin. Utilizing Ioncell fiber provided by the Aalto Ioncell team, plain-woven fabrics were produced and subjected to comprehensive evaluations, including assessments of the mechanical strength, and various tests such as thermal, hydrophobicity, and fractography for the fabricated composites. The Ioncell composite exhibited mechanical strength approximately half that of carbon and glass fibers but surpassed other cellulose fibers. However, thermal degradation in the Ioncell fiber composite occurred earlier than in the carbon fiber composite. SEM images unveiled an exceptional interaction between Ioncell fiber and bio-based epoxy, surpassing other fibers, while contact angle results indicated Ioncell's surface more hydrophobic comparable to that of carbon fiber. Glass transition results demonstrated Ioncell fiber's transformation closely resembling that of the carbon fiber composite since the overall glass transition is controlled by resin which is the major component in our composites. Overall, while some aspects of Ioncell fiber composite may be inferior to carbon, the majority of parameters are comparable, suggesting its potential as a viable, biodegradable alternative in specific applications, emphasizing its environmentally friendly attributes.

Conflicts of interest

The authors confirm that they are not affiliated with or involved in any organization or entity that has a financial or non-financial interest in the subject matter or materials covered in this article.

Acknowledgements

The authors would like to acknowledge the Research Council of Finland's Flagship Programme under Projects No. 318890 and 318891 (Competence Center for Materials Bioeconomy, FinnCERES) for their financial support. All authors are grateful to Aalto University and Bioproduct Technology Group for their support in making this article open-access.

References

1 Dimple, G. P. Singh and R. Mangal, A comprehensive review of natural fiber reinforced composite and their modern application, *Mater. Today: Proc.*, 2023, **92**, 542–548.
2 M. Fazeli, S. Jayaprakash, H. Baniasadi, R. Abidnejad and J. Lipponen, Recycled carbon fiber reinforced composites: Enhancing mechanical properties through co-functionali-

zation of carbon nanotube-bonded microfibrillated cellulose, *Composites, Part A*, 2024, **180**, 1–13.
3 S. Venkatarajan and A. Athijayamani, An overview on natural cellulose fiber reinforced polymer composites, *Mater. Today: Proc.*, 2021, **37**, 3620–3624.
4 GVR - Grand View Research, Cellulose Fiber Market Size, Share & Trends Analysis By Product Type (Natural, Synthetic), By Application (Textile, Hygiene, Industrial), By Regions And Segment Forecasts, 2018–2025, 2016.
5 S. N. Monteiro, F. P. D. Lopes, A. S. Ferreira and D. C. O. Nascimento, Natural-fiber polymer-matrix composites: Cheaper, tougher, and environmentally friendly, *JOM*, 2009, **61**, 17–22.
6 M. A. Azman, M. R. M. Asyraf, A. Khalina, M. Petrů, C. M. Ruzaidi, S. M. Sapuan, W. B. Wan Nik, M. R. Ishak, R. A. Ilyas and M. J. Suriani, Natural fiber reinforced composite material for product design: A short review, *Polymers*, 2021, **13**, 1917.
7 A. K. Das, M. N. Islam, R. K. Ghosh and R. Maryana, Cellulose-based bionanocomposites in energy storage applications-A review, *Heliyon*, 2023, **9**, 13028.
8 M. K. Marichelvam, C. L. Kumar, K. Kandakodeeswaran, B. Thangagiri, K. K. Saxena, K. Kishore, N. K. Wagri and S. Kumar, Investigation on mechanical properties of novel natural fiber-epoxy resin hybrid composites for engineering structural applications, *Case Stud. Constr. Mater.*, 2023, **19**, 1–12.
9 E. M. Yusup, S. Mahzan and M. A. H. Kamaruddin, Natural Fiber Reinforced Polymer for the Application of Sports Equipment using Mold Casting Method, *IOP Conf. Ser.: Mater. Sci. Eng.*, 2019, **494**, DOI: **10.1088/1757-899X/494/1/012040**.
10 H. yan Cheung, M. po Ho, K. tak Lau, F. Cardona and D. Hui, Natural fibre-reinforced composites for bioengineering and environmental engineering applications, *Composites, Part B*, 2009, **40**, 655–663.
11 M. R. M. Zuhair, A. Hamdan and A. R. Irfan, Application of Natural Fibre Composite in the Aviation Industry: A Review, *J. Aviat. Aerosp. Technol.*, 2020, **1**, 1–5.
12 M. Fazeli, F. Fazeli, T. Nuge, O. Abdoli and S. Moghaddam, Study on the Preparation and Properties of Polyamide/Chitosan Nanocomposite Fabricated by Electrospinning Method, *J. Polym. Environ.*, 2022, **30**, 644–652.
13 M. Fazeli, *Development of hydrophobic thermoplastic starch composites*, 2018. **https://pantheon.ufrj.br/handle/11422/7843** (accessed July 17, 2023).
14 M. Fazeli and J. Lipponen, *Developing Self-Assembled Starch Nanoparticles in Starch Nanocomposite Films*, 2022. DOI: **10.1021/acsomega.2c05251**.
15 M. Fazeli, S. Mukherjee, H. Baniasadi, R. Abidnejad, M. Mujtaba, J. Lipponen, J. Seppälä and O. J. Rojas, Lignin beyond the status quo: recent and emerging composite applications, *Green Chem.*, 2024, **26**, 593–630, DOI: **10.1039/D3GC03154C**.
16 N. A. Latip, A. H. Sofian, M. F. Ali, S. N. Ismail and D. M. N. D. Idris, Structural and morphological studies on alkaline pre-treatment of oil palm empty fruit bunch (OPEFB) fiber for composite production, *Mater. Today: Proc.*, 2019, **17**, 1105–1111.
17 Y. G. Thyavihalli Girijappa, S. Mavinkere Rangappa, J. Parameswaranpillai and S. Siengchin, Natural Fibers as Sustainable and Renewable Resource for Development of Eco-Friendly Composites: A Comprehensive Review, *Front. Mater.*, 2019, **6**, DOI: **10.3389/fmats.2019.00226**.
18 M. R. Yazdani McCord, A. Kankkunen, D. Chatzikosmidou, A. Seppälä, J. Seppälä and H. Baniasadi, Polypyrrole-modified flax fiber sponge impregnated with fatty acids as bio-based form-stable phase change materials for enhanced thermal energy storage and conversion, *J. Energy Storage*, 2024, **81**, 110363, DOI: **10.1016/j.est.2023.110363**.
19 S. Dahiya, R. Katakojwala, S. Ramakrishna and S. V. Mohan, Biobased Products and Life Cycle Assessment in the Context of Circular Economy and Sustainability, *Mater. Circ. Econ.*, 2020, **2**, 2–7.
20 A. K. Bledzki, A. Jaszkiewicz and D. Scherzer, Mechanical properties of PLA composites with man-made cellulose and abaca fibres, *Composites, Part A*, 2009, **40**, 404–412.
21 M. R. Sanjay, G. R. Arpitha, P. Senthamaraikannan, M. Kathiresan, M. A. Saibalaji and B. Yogesha, The Hybrid Effect of Jute/Kenaf/E-Glass Woven Fabric Epoxy Composites for Medium Load Applications: Impact, Inter-Laminar Strength, and Failure Surface Characterization, *J. Nat. Fibers*, 2019, **16**, 600–612.
22 W. Gindl and J. Keckes, Strain hardening in regenerated cellulose fibres, *Compos. Sci. Technol.*, 2006, **66**, 2049–2053.
23 K. Yorseng, S. M. Rangappa, H. Pulikkalparambil, S. Siengchin and J. Parameswaranpillai, Accelerated weathering studies of kenaf/sisal fiber fabric reinforced fully bio-based hybrid bioepoxy composites for semi-structural applications: Morphology, thermo-mechanical, water absorption behavior and surface hydrophobicity, *Constr. Build. Mater.*, 2020, **235**, 108–127.
24 H. Santamala, R. Livingston, H. Sixta, M. Hummel, M. Skrifvars and O. Saarela, Advantages of regenerated cellulose fibres as compared to flax fibres in the processability and mechanical performance of thermoset composites, *Composites, Part A*, 2016, **84**, 377–385.
25 M. Fazeli, X. Liu and C. Rudd, The effect of waterborne polyurethane coating on the mechanical properties of epoxy-based composite containing recycled carbon fibres, *Surf. Interfaces*, 2022, **29**, 101684, DOI: **10.1016/j.surfin.2021.101684**.
26 P. Khalili, M. Skrifvars and A. S. Ertürk, Fabrication, Mechanical Testing and Structural Simulation of Regenerated Cellulose Fabric Elium® Thermoplastic Composite System, *Polymers*, 2021, **13**, 2969.
27 U. Koc, Y. Aykut and R. Eren, Regenerated cellulose woven fabric reinforced hydrogel composite, *J. Text. Inst.*, 2022, **113**, 906–914.
28 A. Karakoc, M. Bulota, M. Hummel, S. Sriubaitė, M. Hughes, H. Sixta and J. Paltakari, Effect of single-fiber properties and fiber volume fraction on the mechanical

properties of Ioncell fiber composites, *J. Reinf. Plast. Compos.*, 2021, **40**, 741–748.
29 M. R. Sanjay, P. Madhu, M. Jawaid, P. Senthamaraikannan, S. Senthil and S. Pradeep, Characterization and properties of natural fiber polymer composites: A comprehensive review, *J. Cleaner Prod.*, 2018, **172**, 566–581.
30 Y. Yang, D. Chen, Y. Cheng, B. Sun, G. Zhao, W. Fei, W. Han, J. Han and X. Zhang, Eco-friendly and sustainable approach of assembling sugars into biobased carbon fibers, *Green Chem.*, 2022, **24**, 5097–5106.
31 S. M. Rangappa, S. Siengchin, J. Parameswaranpillai, M. Jawaid and T. Ozbakkaloglu, Lignocellulosic fiber reinforced composites: Progress, performance, properties, applications, and future perspectives, *Polym. Compos.*, 2022, **43**, 645–691.
32 H. Sixta, A. Michud, L. Hauru, S. Asaadi, Y. Ma, A. W. T. King, I. Kilpeläinen and M. Hummel, Ioncell-F: A high-strength regenerated cellulose fibre, *Nord. Pulp Pap. Res. J.*, 2015, **30**, 043–057.
33 S. Asaadi, T. Kakko, A. W. T. King, I. Kilpeläinen, M. Hummel and H. Sixta, High-Performance Acetylated Ioncell-F Fibers with Low Degree of Substitution, *ACS Sustainable Chem. Eng.*, 2018, **6**, 9418–9426.
34 A. Michud, M. Tanttu, S. Asaadi, Y. Ma, E. Netti, P. Kääriainen, A. Persson, A. Berntsson, M. Hummel and H. Sixta, Ioncell-F: ionic liquid-based cellulosic textile fibers as an alternative to viscose and Lyocell, *Text. Res. J.*, 2016, **86**, 543–552.
35 M. Rissanen, I. Schlapp-Hackl, D. Sawada, S. Raiskio, K. Ojha, E. Smith and H. Sixta, Chemical recycling of hemp waste textiles via the ionic liquid based dry-jet-wet spinning technology, *Text. Res. J.*, 2023, **93**, 2545–2557.
36 R. R. Mather and R. H. Wardman, *Chemistry of Textile Fibres*, Royal Society of Chemistry, 2nd edn, 2015.
37 M. Rejeb, A. Koubaa, F. Elleuch, F. Godard, S. Migneault, M. Khlif and H. Mrad, Effects of coating on the dimensional stability of wood-polymer composites, *Coatings*, 2021, **11**, 711.
38 H. Baniasadi, J. Trifol, S. Lipponen and J. Seppälä, Sustainable composites of surface-modified cellulose with low–melting point polyamide, *Mater. Today Chem.*, 2021, **22**, 1–13.
39 A. Atmakuri, A. Palevicius, M. Siddabathula, A. Vilkauskas and G. Janusas, Analysis of mechanical and wettability properties of natural fiber–reinforced epoxy hybrid composites, *Polymers*, 2020, **12**, 2827.
40 E. Bormashenko and Y. Bormashenko, Wetting of composite surfaces: When and why is the area far from the triple line important?, *J. Phys. Chem. C*, 2013, **117**, 19552–19557.
41 N. M. Nurazzi, M. R. M. Asyraf, M. Rayung, M. N. F. Norrrahim, S. S. Shazleen, M. S. A. Rani, A. R. Shafi, H. A. Aisyah, M. H. M. Radzi, F. A. Sabaruddin, R. A. Ilyas, E. S. Zainudin and K. Abdan, Thermogravimetric analysis properties of cellulosic natural fiber polymer composites: A review on influence of chemical treatments, *Polymers*, 2021, **13**, 2710.
42 B. Z. Marchi, P. H. P. M. da Silveira, W. B. A. Bezerra, L. F. C. Nascimento, F. P. D. Lopes, V. S. Candido, A. C. R. da Silva and S. N. Monteiro, Ballistic Performance, Thermal and Chemical Characterization of Ubim Fiber (Geonoma baculifera) Reinforced Epoxy Matrix Composites, *Polymers*, 2023, **15**, 3220.
43 F. Wang, M. Lu, S. Zhou, Z. Lu and S. Ran, Effect of fiber surface modification on the interfacial adhesion and thermo-mechanical performance of unidirectional epoxy-based composites reinforced with bamboo fibers, *Molecules*, 2019, **24**, 2682.
44 J. Trifol, S. Jayaprakash, H. Baniasadi, R. Ajdary, N. Kretzschmar, O. J. Rojas, J. Partanen and J. V. Seppälä, 3D-Printed Thermoset Biocomposites Based on Forest Residues by Delayed Extrusion of Cold Masterbatch (DECMA), *ACS Sustainable Chem. Eng.*, 2021, **9**, 13979–13987.
45 K. Naito, Effect of strain rate on tensile properties of carbon fiber epoxy-impregnated bundle composite, *J. Mater. Eng. Perform.*, 2014, **23**, 708–714.
46 H. Baniasadi, S. Lipponen, M. Asplund and J. Seppälä, High-concentration lignin biocomposites with low-melting point biopolyamide, *Chem. Eng. J.*, 2023, **451**, 138564.
47 H. Baniasadi, Z. Madani, M. Mohan, M. Vaara, S. Lipponen, J. Vapaavuori and J. V. Seppälä, Heat-Induced Actuator Fibers: Starch-Containing Biopolyamide Composites for Functional Textiles, *ACS Appl. Mater. Interfaces*, 2023, **15**, 48584–48600, DOI: **10.1021/acsami.3c08774**.
48 M. Bulota, S. Sriubaite, A. Michud, K. Nieminen, M. Hughes, H. Sixta and M. Hummel, The fiber-matrix interface in Ioncell cellulose fiber composites and its implications for the mechanical performance, *J. Appl. Polym. Sci.*, 2021, **138**, 1–8.